nature climate change

SUPPLEMENTARY INFORMATION

DOI: 10.1038/NCLIMATE2060

Continued global warming after CO_2 emissions stoppage

Thomas Lukas Frölicher[1,2*] Michael Winton[3] Jorge Louis Sarmiento[1]

[1] Environmental Physics, Institute of Biogeochemistry and Pollutant Dynamics, ETH Zürich, Zürich, Switzerland

[2] Program in Atmospheric and Oceanic Sciences, Princeton University, Princeton, USA

[3] Geophysical Fluid Dynamics Laboratory, Princeton, USA

Comparison between modeled and observational-based equilibrium climate sensitivity and radiative forcing estimates for a doubling of atmospheric CO_2

We applied the 'Gregory method'[1] for calculating the equilibrium climate sensitivity (T_{eq} ($2xCO_2$)) and radiative forcing for a doubling of CO_2 to 150 years of ocean heat uptake and global mean surface temperature data taken from abrupt CO_2 quadrupling experiments with the ESM2M and CSM1. Similarly, Andrews et al. (2012)[2] applied the Gregory method to abrupt CO_2 quadrupling experiments from the CMIP5 ensemble. The Gregory method is based on the simple standard "zero-layer" energy balance model of the climate system, which does not include ocean heat uptake efficacy:

$$\Delta T(t) = \frac{R(t) - N(t)}{\lambda}. \quad \text{(S1)}$$

ΔT is the global mean surface temperature change, R is the stratospheric adjusted radiative forcing, N is the net radiation flux at top-of-the-atmosphere or ocean heat uptake (on decadal and longer time scales), and λ is the equilibrium climate feedback factor. If R (for constant $4xCO_2$) and λ are constant, N is a linear function of ΔT with a slope of $1/\lambda$ and intercept of R/λ (equal to T_{eq} ($2xCO_2$)). Therefore, both R and λ can be calculated by linear regression.

The small black points in Figure S3a-b show the relationship between ocean heat uptake and temperature simulated by the ESM2M (Fig. S3a) and CSM1 (Fig. S3b) for the abrupt CO_2 quadrupling experiment. The x-intercept and the y-intercept of the regression fits shown as large black points indicate the Gregory equilibrium climate sensitivity estimates (labeled as 'T_{eq} ($2xCO_2$)') and radiative forcing estimates (labeled as 'R ($2xCO_2$)') for a doubling of CO_2, respectively. The large red (ESM2M, Fig. S3a) and blue (CSM1, Fig. S3b) points indicate equilibrium climate sensitivity and radiative forcing estimates based on the carbon pulse experiments. The red (ESM2M) and blue (CSM1) crosses in Figure S3a-b are alternative equilibrium climate sensitivity and radiative forcing estimates based on atmospheric/slab-ocean[4,5] and radiative transfer code experiments.

The Gregory method (2.4K, large black point at x-intercept in Fig. S3a) underestimates the ESM2M $2xCO_2$ equilibrium climate sensitivity calculated from our carbon pulse experiments (3.1K, large red point at x-intercept in Fig. S3a). The equilibrium climate sensitivity estimates from our carbon pulse experiment, however, are in good agreement with the atmosphere/slab ocean configurations of the same model[3] (3.4K, large red cross at x-intercept in Fig. S3a). The Gregory method (3.4 Wm^{-2}, large black point at y-intercept in Fig. S3a) also slightly underestimates the $2xCO_2$ radiative forcing estimated using the simplified expression $R = 5.35 \bullet \ln(CO_2(t)/CO_2(t=0))$ (3.7 Wm^{-2}, large red point at y-intercept in Fig. S3a) and the radiative forcing estimated using the radiative transfer code[3] (3.5 Wm^{-2}, large red cross at y-intercept in Fig. S3a).

The Gregory $2xCO_2$ equilibrium climate sensitivity of 2.1K for CSM1 (large black point at x-intercept in Fig. S3b) is in good agreement with the $2xCO_2$ equilibrium climate sensitivity of 2.0K from our carbon pulse experiments (large blue point at x-intercept in Fig. S3b) and $2xCO_2$ equilibrium climate sensitivity of 2.1K from the atmosphere/slab ocean configuration[4] (blue cross at x-intercept in Fig. S3b), but the Gregory $2xCO_2$ radiation forcing of 2.7 W m^{-2} (black point at y-intercept in Fig. S3b) largely underestimates the CSM1 $2xCO_2$ radiative forcing estimated using the simplified expression of 3.7 W m^{-2} (large blue point at y-intercept in Fig. S3b) and estimated using the radiative transfer code[4] of 3.5 Wm^{-2} (blue cross at y-intercept in Fig. S3b).

Figure S3c compares recent observational-based estimates of equilibrium climate sensitivity and transient climate response (the temperature response at CO_2 doubling following a 1% yr^{-1} CO_2 increase; labeled with 'TCR' in Fig. S3c) with estimates obtained from ESM2M (red points in Fig. S3c) and CMIP3 models. Small green points in Fig. S3c show individual CMIP3 models and large green points in Fig S3c show CMIP3 multi-model mean estimates[1]. Otto et al. (2013)[5] used observation-based estimates (labeled with 'observations' in Fig S3c) of global mean surface temperature, ocean heat uptake and radiative forcing over the most recent decade 2000-2009 relative to 1860-1879 to obtain the slope $1/\lambda$ in the ocean heat uptake-temperature relationship. They then estimated (labeled with 'scaled observations' in Fig. S3c) a equilibrium climate sensitivity of 2.0K (large black point at x-intercept in Fig. S3c) and a transient climate response of 1.3K (large black point labeled with 'TCR' in Fig. S3c) to a doubling of atmospheric CO_2 by assuming a radiative forcing of $3.44W/m^2$ for a doubling of CO_2. Both, the ESM2M (TCR=1.5K) and the observations (TCR=1.3K) indicate a relatively small transient climate response. The ESM2M equilibrium climate sensitivity of 3.1 K, however, is significantly larger than the 2.0 K obtained from observations because of the kink in the evolution of the climate change state along its path to equilibrium. The kink is caused by the non-unity ocean heat uptake efficacy. The CMIP3 models as a class also indicate a kink in the evolution of the climate change state (green lines in Fig. S3c).

Calculations of impulse response function

The impulse response function, or Green's function, of atmospheric CO_2 represents the fraction of the enhancement in atmospheric CO_2 due to the added carbon emission pulse, which remains in the atmospheric at time t. The impulse response function of atmospheric CO_2 is fitted by a sum of exponentials:

(S2) $IRF(t) = a_0 + \sum_{i=1}^{3} a_i \cdot \exp\left(\frac{-t}{\tau_i}\right)$ for $0 \leq t \leq 1000$yr

The conditions are applied that the sum of the coefficients a_i equals one.

The mean relative error, mre, is calculated according to:

(S3) $mre = \frac{1}{1000} \cdot \sum_{i=1}^{1000} \frac{f_i - m_i}{m_i}$,

where f_i are the annual airborne fraction data from the fit and m_i from the model output. Values are given in Table S2.

Supplementary References:

1. Gregory, J. M., et al., A new method for diagnosing radiative forcing and climate sensitivity. *Geophys. Res. Lett.*, **31**, L03205 (2004).

2. Andrews, T., J. M. Gregory, M. J. Webb, K. E. Taylor, Forcing, feedbacks and climate sensitivity in CMIP5 coupled atmosphere-ocean climate models. *Geophys. Res. Lett,* **39**, L09712 (2012).

3. Delworth, T. L., et al., GFDL's CM2 global coupled climate models. Part I: Formulation and Simulation Characteristics. *J. Climate*, **19**, 643-674 (2006).

4. Meehl, G. A., et al., Response of the NCAR climate system model to increased CO_2 and the role of physical processes. *J. Climate*, **13**, 1879-1898 (2000).

5. Otto, A., et al., Energy budget constraints on climate response. *Nat. Geosci*., **6**, 415-416 (2013).

6. Winton, M. Takahashi, K., I. M. Held, Importance of ocean heat uptake efficacy to transient climate change. *J. Climate*, **23**, 2333-2344 (2010).

Supplementary Table S1: **Efficacy ε, equilibrium climate feedback parameter λ, and equilibrium climate sensitivity T_{eq} ($2xCO_2$) for the ESM2M and CSM1 using the carbon pulse experiment.**

Model	ε	λ ($W\ m^{-2}\ K^{-1}$)	T_{eq} ($2xCO_2$) (K)
ESM2M (ensemble 1, 1000-yr long)	1.87	1.19	3.12
ESM2M (ensemble 2, 600-yr long)	1.78	1.24	2.99
CSM1 (1000-yr long)	1.65	1.90	1.95

Supplementary Table S2: **Coefficients to fit the response of the simulated airborne fraction in ESM2M and CSM1 to a pulse emission of 1800 GtC following equation S2.** The timescales τ_i are given in years. The mean relative error (mre) is given in percent. The parameters for the two-model mean are also given.

Model	*mre*	a_0	a_1	a_2	a_3	τ_1	τ_2	τ_3
ESM2M	0.8	0.181	0.205	0.385	0.230	392	35.3	3.166
CSM1	0.4	0.186	0.236	0.446	0.132	475	35.2	4.431
mean	0.5	0.184	0.220	0.416	0.180	433	35.3	3.577

Supplementary Figure S1: Changes in carbon pools. Time series of atmosphere (red lines), land (green lines) and ocean (blue lines) carbon inventory simulated by (a) the ESM2M and (b) the CSM1.

Supplementary Figure S2: Influence of ocean heat uptake efficacy on global mean temperature responses in ESM2M and CSM1. Time series of simulated temperature responses (black lines), and estimated temperature responses using the simulated radiative forcing, ocean heat uptake and equilibrium climate feedback parameter from the two models, but inserting the efficacies from the ESM2M (1.87; red lines), the CSM1 (1.65; blue lines) and the multi-model mean from the CMIP3 models[2] (1.34; gray lines) in equation (1). The error bars correspond to the extreme values of efficacy in CMIP3 models (0.74 and 1.99). The time series are smoothed with a 20-yr running mean. Only the first 500 years are shown, as the product εN is close to zero afterwards. If the simplified zero order energy balance model (equation 1) would work perfectly, the estimated temperature (red line in (a) and blue line in (b)) would be equal to the actual simulated temperature (black lines in (a) and (b)).

Supplementary Figure S3: Relationships between the change in net top-of-atmosphere radiation (or ocean heat uptake) and global mean surface air temperature. (a,b) Small black points show simulated changes in (a) ESM2M and (b) CSM1 from a 150-yr instantaneous $4xCO_2$ experiment with constant prescribed CO_2. Data points are global-annual means and results are scaled for a doubling of CO_2. Black lines represent ordinary least square regressions fits to the 150 years of data. The x-intercept represents equilibrium climate sensitivity estimates (labeled as 'T_{eq} ($2xCO_2$)') and the y-intercept represents radiative forcing estimates (labeled as 'R ($2xCO_2$)')

for a doubling of CO_2. Equilibrium climate sensitivity and radiative forcing estimates for a doubling of CO_2 obtained from our carbon pulse experiments, from the atmosphere/slab-ocean model configuration and from the radiative transfer code are also shown as large points and crosses. (c) Comparison of transient climate response (labeled as 'TCR') and equilibrium climate sensitivity between observational-based estimates[3] and modeled estimates from the ESM2M and CMIP3 models. The observational-based changes (indicated with 'observations') in radiative forcing, global mean temperature and total ocean heat uptake represent estimates over the most recent decade 2000-2009 relative to 1860-1879[5]. Equilibrium climate sensitivity and radiative forcing estimates for a doubling of CO_2 for ESM2M are taken from our carbon pulse experiments. All transient climate response estimates and CMIP3 model results are taken from Table 2 of Winton et al.[6]. Transient climate responses were calculated using the differences between 20-yr averages taken at CO_2 doubling from a 1% CO_2 increase experiment, and a 140-yr period, centered on the time of doubling, from the control simulations[6]. CSM1 is missing in (c) as the 1% CO_2 increase experiment was not available.

Supplementary Figure S4: Simulated efficacies. Scatterplot of one minus scaled simulated global mean temperature (1- $T(t)/T_{eq}(t)$) against simulated TOA net heat flux ($N(t)/R(t)$). According to equation $\frac{N(t)}{R(t)} = \frac{1}{\varepsilon} \cdot (1 - \frac{\Delta T(t)}{\Delta T_{eq}(t)})$, the slope of the lines emphasize the efficacy. All points are centennial averages.

Supplementary Figure S1:

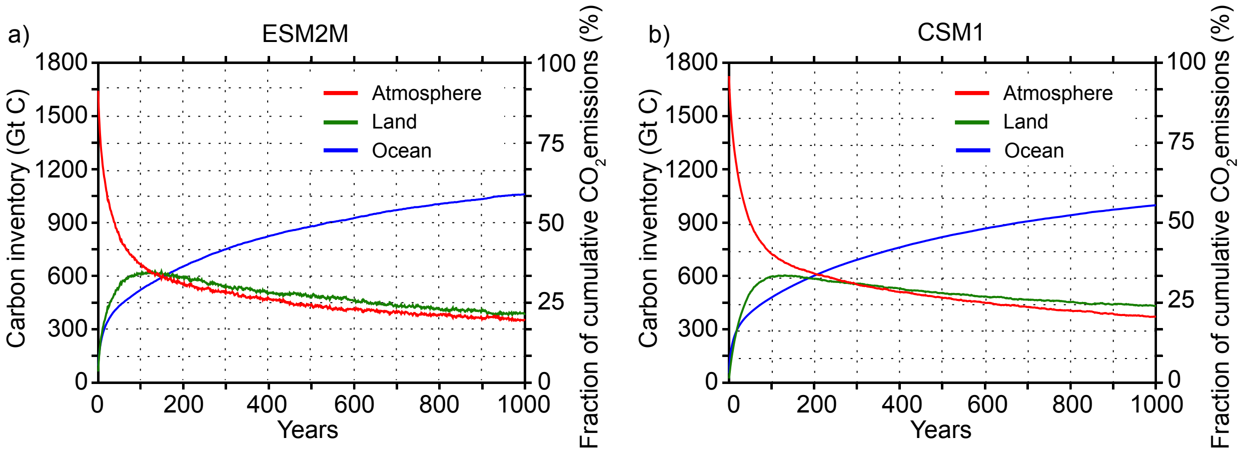

Supplementary Figure S2:

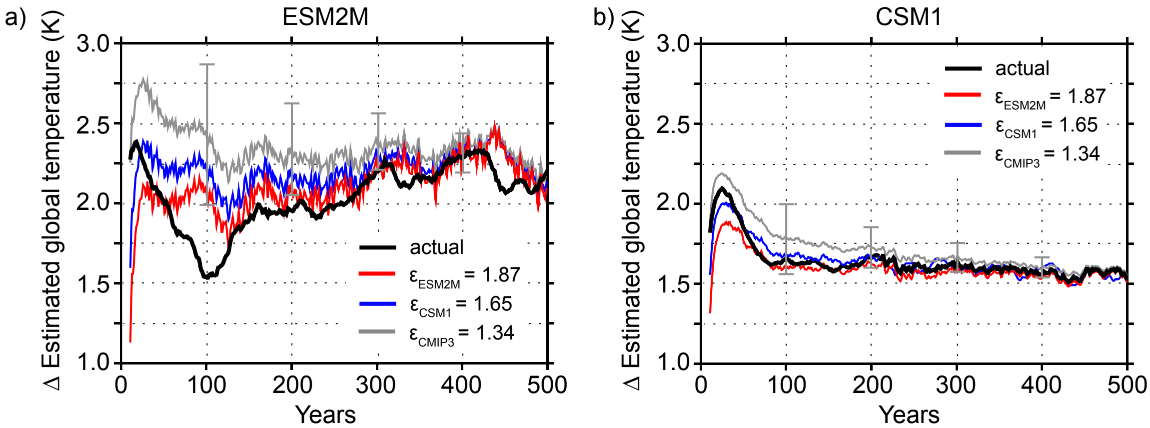

Supplementary Figure S3:

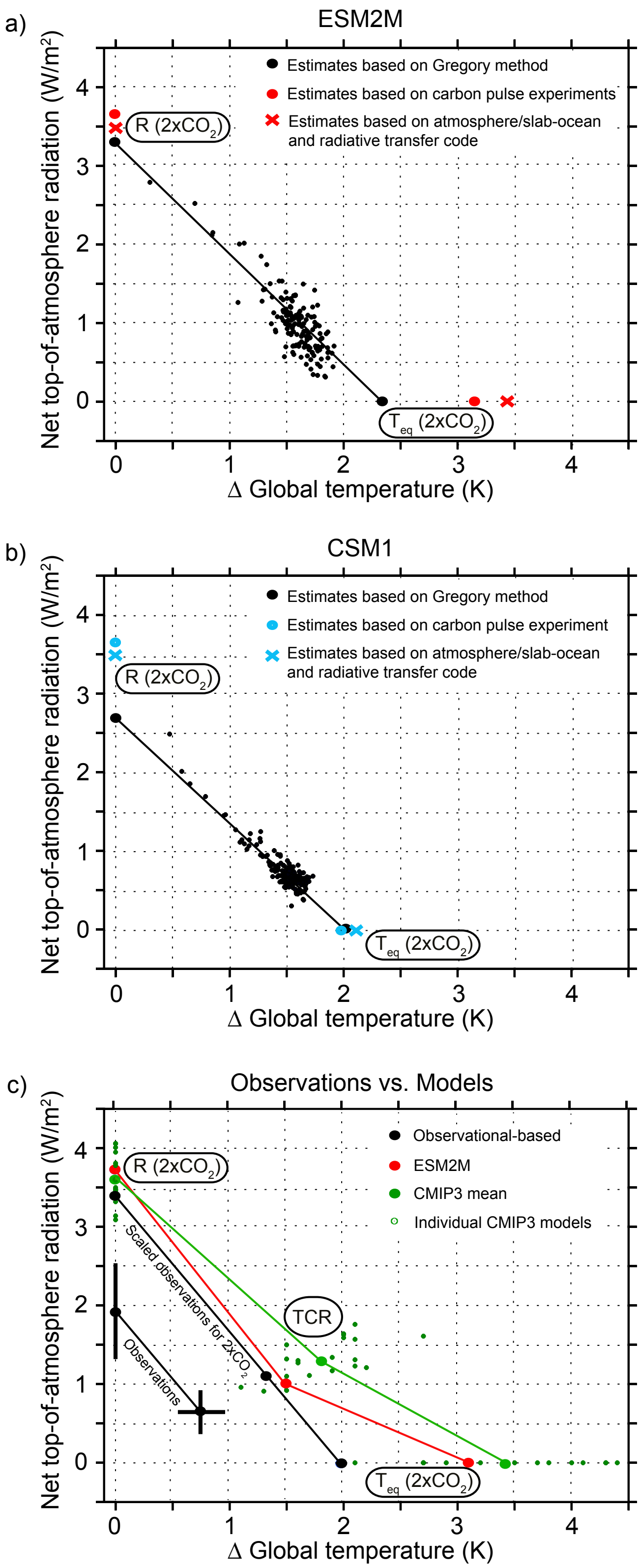

163 **Supplementary Figure S4:**

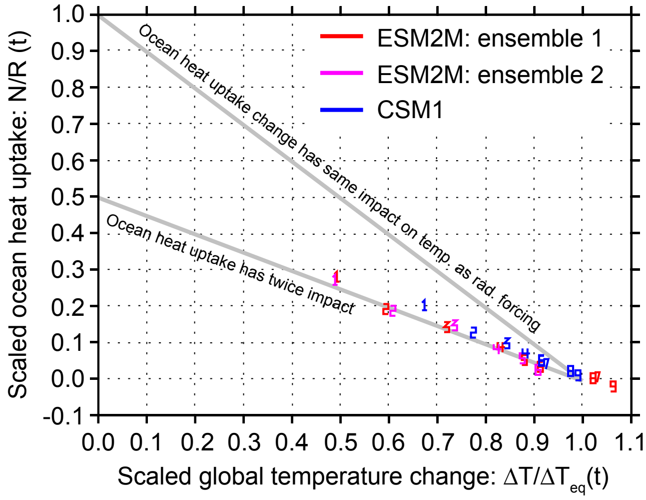

164